Candidate NAMPT modulators from traditional African, Chinese, and Russian medicinal plants

Jarmila Nahálková,*[a]

[a] – Biochemistry, Molecular, and Cell Biology Unit, Biochemworld Co.; Snickar-Anders väg 17, 74394, Skyttorp, Uppsala County, Sweden; Mobile: +46 73 7707700; E-mail: jarmila.nahalkova@biochemworld.net; ORCID ID: https://orcid.org/0000-0001-9918-6105

* - corresponding author

Abstract

The mitochondrial bioenergetics hypothesis postulates a critical role of mitochondrial activity in aging, which leads to the development of age-related diseases if disturbed. NAD+ and NADH generate a powerful oxidoreductive system driving ATP production in mitochondria, therefore, the maintenance of the NAD+/NADH ratio is crucial for the metabolic homeostasis in cells. The activation of nicotinamide phosphoribosyl transferase (NAMPT) is a superior approach to increase cellular levels of NAD+ since it is a rate-limiting enzyme of NAD+ salvage pathway producing NAD+ precursor nicotinamide mononucleotide. NAMPT inhibitors are, however, also desired by pharmaceutical applications due to their potency in limiting the growth of cancer cells. The present work demonstrates an in-silico approach for screening NAMPT activity modulators using compound libraries from traditional African, Chinese, and Russian medicinal plants. The compounds predicted to pass the blood-brain barrier, with low predicted toxicity and desirable pharmacokinetic and drug-likeness characteristics, were subjected to further selection by molecular docking using CB-Dock2. A panel of 21 compounds, including known NAMPT

activators, inhibitors, negative controls, and randomly chosen compounds, was used to validate the docking method. The selection yielded 17 compounds with increased docking scores when tested against 6 co-crystallized structures of NAMPT. Their 2D protein-ligand interactions were critically evaluated and correlated with known interactions of the NAMPT activators and inhibitors with the active and allosteric sites of the enzyme. The selected compounds are suitable for the experimental pharmaceutical developments of drugs for aging, neurological diseases, and cancer treatments.

Keywords: NAMPT; NAD^+/NADH; neurodegeneration; cancer; virtual screening

Abbreviations: AA – amino acid; AD – Alzheimer´s disease; ALS – amyotrophic lateral sclerosis; BBB – blood-brain barrier; BIOVIA DSV – Biovia Discovery Studio Visualizer; ETC – electron transfer chain; HD – Huntington´s disease; NAM – nicotinamide; NAMPT – nicotinamide phosphoribosyltransferase; NMN – nicotinamide mononucleotide; PD – Parkinson´s disease; VDW – Van der Waals

1. Introduction

Decades of research dedicated to mitochondrial functions led to the development of the "mitochondrial bioenergetics hypothesis" built on the significant contribution of mitochondrial fitness to aging and age-related diseases. They contribute by energy manufacture, production, and detoxification of reactive oxygen species to the most essential cellular functions.

Mitochondria produce a proton flow from the proton pumps of the respiratory chain complexes I, II, and IV located on the inner mitochondrial membrane and driven by the electron flow from NADH to oxygen followed by the regeneration of NAD^+. The protons exported from the mitochondrial matrix to the intermembrane space create membrane potential, which drives their re-entry back to the mitochondrial matrix through ATP synthase generating ATP from ADP [1]. Since the complex I of the electron transport chain (ETC) is involved in cellular energy production and NAD^+ regeneration, accordingly, it contributes to the maintenance of the NAD^+/NADH ratio important for cellular homeostasis. The ratio decreases during the process of aging probably due to the increased NAD^+ consumption by PARP-s and CD38 in combination with the NAD^+ production decline [2]. The age-dependent depletion of NAD^+ is particularly linked to Alzheimer´s disease (AD), Parkinson´s disease (PD), Huntington´s disease (HD), and amyotrophic lateral sclerosis (ALS) pathologies. Increasing its levels can inhibit the occurrence of these pathologies in animal models [2]. Supplementing of NAD^+ precursors and/or the inhibition of NAD^+-consuming proteins has a neuroprotective effect against the mitochondrial defects of PD models of *D. melanogaster* [3]. Increasing NAD^+ production positively affects 10 hallmarks of aging [2] [4], which demonstrates the importance of the maintenance of NAD^+ for healthy aging and the prevention of the associated diseases.

The activation of nicotinamide phosphoribosyltransferase (NAMPT) is a superior approach to increase the NAD^+/NADH ratio in the cells and in this way stimulate cellular bioenergetics decline during aging. NAMPT was originally purified and characterized in 1957 as an enzyme producing nicotinamide mononucleotide (NMN) from nicotinamide (NAM) by transfer of ribosyl pyrophosphate group of 5-phosphoribosyl 1-pyrophosphate (PPRP) [5]. NMN is then converted to NAD^+ by nicotinamide dinucleotide adenylyl transferase (NMNAT) [6,7]. NAMPT

is a rate-limiting enzyme of NAD^+ biosynthesis by salvage of NAM produced by NAD^+ catabolism of NAD^+-dependent proteins with NAD-ase activity such as SIRT-s, PARP-s and CD38 [8].

Interestingly, the anti-aging and lifespan-extending effect was achieved by the supplementation of NAMPT-containing extracellular vesicles to the experimental mice [9]. The relevance of the enzyme to the pathology of neurodegenerative disease was demonstrated by the deletion of NAMPT in projection neurons, which triggered mitochondrial and synaptic dysfunctions and further caused neurodegeneration specifically located in the motor cortex. It was also accompanied by muscular atrophy and gradual paralysis, loss of brown adipose tissue (BAT), and shortened lifespan, which was partially rescued by nicotinamide mononucleotide (NMN) in diet [10]. The dopaminergic neurons are more vulnerable to NAMPT depletion, which leads to Parkinson´s disease-like symptoms in mice [11]. The homozygous NAMPT deficiency in mice is lethal at the prenatal stage, however, heterozygous deficient animals survive rather normally with decreased intracellular levels of NAMPT in body tissues. A possible explanation is the balancing of NAD^+ levels by *de novo* synthesis through the tryptophan kynurenine pathway. Defects caused by NAD^+ deficiency can also be reverted by the supply of NMN in the experimental animals [12].

In animal models of AD, improvement of memory impairment and inhibition of Tau phosphorylation was accomplished by the induction of mitophagy [13]. Significantly, NAD^+ precursor NMN is one of the powerful inducers of mitophagy [14] and it can occur by multiple mechanisms, which include NAD^+ dependent proteins SIRT1, SIRT3, SIRT6, SIRT7, SARM1, CD38, IL-1, and more [15]. Mitophagy stimulation by NMN is considered a therapeutical target for AD, therefore NAMPT activators should be beneficial for pharmacological purposes.

Increased NAD^+ levels were also observed as a consequence of the calorie restriction (CR), which was accompanied by increased SIRT1 expression and SIRT1-mediated activation of α-secretase [16]. Enzymes participating in different steps of NAD^+ biosynthetic pathway including NAMPT protect axonal functions in cultured dorsal root ganglion neurons. Similarly, NAD^+ and its precursors NAM and NMN also have protective effects on axons [17]. β-amyloid plaque load and ATP levels significantly improved both in the cortex and hippocampus by administration of NAD^+ to APPswe/PS1 ΔE9 animal model [18]. Protein expressions of NAMPT and SIRT1 in the cortex and hippocampus are decreased in APPswe/PS1 ΔE9 mice, which can be reversed by administration of NAD^+ [18, 19]. NAD^+/NADH ratio is also lower compared to control brains in this mouse model [18]. Since NAD^+ levels and NAD^+/NADH are decreased in these mice after administration of NAMPT inhibitor FK866 treatment, it can be concluded, that NAD^+ levels are generated through salvage pathway via NAMPT [20]. Therefore, the activation of brain NAMPT can provide benefits for AD treatment.

NAMPT inhibitors are also desired due to their potency to limit the growth of cancer cells [21]. Low-toxic NAMPT modulators able to penetrate the blood-brain (BBB) barrier with desirable pharmacokinetic characteristics should be pharmacologically beneficial. The present work shows an *in-silico* approach for screening such types of modulators of NAMPT activity using compounds from traditional African, Chinese, and Russian medicinal plant libraries.

2. Materials and methods

Collection of bioactive compounds: The potential NAMPT modulators were collected from libraries of bioactive compounds originating from African medicinal plants [22–24]. As a second source of the potential NAMPT modulators was used a server for the drug repurposing DrugRep,

which is based on a compound library of traditional Chinese medicinal plants [25]. The DrugRep receptor-based screen was run using traditional Chinese, FDA experimental drug, and FDA-approved drug libraries. Input included co-crystallized NAMPT with the substrate NAM (PDB: 8DSI); NAM and the activator NP-A1-R (TIE) (PDB: 8DSC); NAM and the activator quercitrin (PDB: 8DSE); and NAM and the activator NAT 2-(2-tert-butylphenoxy)-N-(4-hydroxyphenyl) (PDB: 7ENQ). Compounds with better docking scores than -9 kcal/mol were collected for further selection. A compound from Russian traditional medicine ononetin was also tested since it is mentioned in the literature as a NAMPT modulator, but the evidence is missing [26].

Virtual compound screening: The pharmacological properties of 191 compounds from African medicinal plants and 40 compounds from DrugRep screening were assessed by SwissADME [27]. Predicted BBB permeability was prioritized at this stage of the screening and compounds not fulfilling this criterium were excluded before assessment of other pharmacological properties. Their toxicities were predicted by ProTox-II, a webserver for the prediction of the toxicity of chemicals [28]. Selected compounds were further screened by molecular docking using the docking tool CB-Dock2 [29] by docking into the structures obtained from Protein Data Bank (PDB; http://www.pdb.org) [30] including 8DSI [31], 8DSE [31], 8DSC [31] and 7ENQ [32]. Two NAMPT structures co-crystallized with inhibitors GNE-618 (PDB: 4o13) [33], and 5-nitro-1H-benzimidazole (2ZM, PDB: 4N9C) [34] were also included to monitor inhibitor-specific protein-ligand interactions. The molecular docking analyses were repeated twice and the average value is presented. The schema of the workflow of the virtual NAMPT modulator screening was created by Adobe Illustrator 2025.

Protein-ligand interaction analysis: The analysis of the protein-ligand interactions was performed using 2D diagrams of the interactions between the compounds and the active and

allosteric sites of NAMPT. PDB files downloaded from the molecular docking application CB-Dock2 were visualized by a 2D diagram of BIOVIA Discovery Studio Visualizer (DSV) v.24.1.0.23298 and compared with the known interactions of control compounds (NAMPT activators and inhibitors). The method assisted in the validation of the molecular docking method and for the characterization of the binding of new compounds with potential modulatory effects on NAMPT activity.

Chemical structure similarity network: The network was constructed by importing the list of the compounds containing their names and smile identifiers as a comma-delimited CSV-UTF8 (*.csv) file. The data were imported as a network from the file to Cytoscape v 3.10.2 [35] and analyzed by the cheminformatics application ChemViz2 v.2.0.3 [36]. The Cheminformatics Tools application run was used to construct a chemical structure similarity network and to export the pharmacokinetic parameters of the selected compounds. The results were created using a Prefuse force-directed layout, where the node distance and a number of the common links define the structural similarity in a fingerprint-like manner.

3. Results

The main goal of the present study is to find candidate modulators of NAMPT activity among compounds from traditional African, Chinese, and Russian medicinal plants. Activators could be used for the improvement of mitochondrial bioenergetics during normal aging and/or for the improvement of conditions of patients with neurodegenerative diseases (AD, PD, HD, ALS) by increasing the cellular NAD^+/NADH ratio. The inhibitors of NAMPT are also potentially valuable since they are wanted for the treatment of cancer patients.

As a basic source of the naturally occurring compounds were used libraries originated from African medicinal plants [22–24], which included a pan-African natural product library (p-ANAPL) [22]; a library of bioactive compounds from central African flora [23] and a database of phytochemicals from medicinal plant *Kigelia africana*. A second source of potential NAMPT modulators was a server for drug repurposing DrugRep based on a compound library of traditional Chinese medicinal plants [25]. An additional compound ononetin originated from the Russian traditional medicinal plant *Ononis spinosa* [26] was also included among candidates.

The list of 231 natural compounds was subjected to pharmacological screening using SwissADME developed by the Swiss Institute of Bioinformatics for the prediction of the pharmacokinetic characteristics, medicinal chemistry friendliness, and drug-likeness of the candidate compounds [27]. As the first selection criterium was used the predicted ability to penetrate BBB to be capable of affecting brain functions (Fig. 1). Characteristics as high gastrointestinal absorption (GI), at least moderate water solubility based on SILICOS-IT method (SILICOS-IT: Fragmental method calculates by FILTER-IT program, version 1.0.2; http://www.silicos-it.be) and breaking maximum one Lipinski´s rules were applied as the next selection criteria of the screening. The compounds fulfilling these basic pharmacological measures were further subjected to toxicity prediction using Pro-Tox II [28], which aimed to exclude highly toxic compounds.

In general, molecular docking methods suffer from bias towards the high molecular weight and lipophilicity of the ligands [37]. Here, the highly lipophilic and high molecular weight compounds were already excluded after the first assessment of BBB permeability, since only water-soluble or moderately water-soluble compounds with M_r<500 g/mol were selected for further screening. All new candidate NAMPT modulators have M_r in the range 318-416 g/mol.

The molecular docking executed by the user-friendly platform CB-Dock2 [29] (Fig. 1) yielded 17 compounds above the chosen threshold of -9 kcal/mol. Their scores were better compared to the negative control compounds and comparable with positive controls (NAMPT activators and inhibitors).

3.1 Validation of the molecular docking method

Molecular docking methods are known to have low consistency, therefore extensive validation is required to increase the reliability. CB-Dock2 developers promise 85 % accuracy of the obtained results [29], which could provide a good starting point for low-cost bioactive compound screening. The ambition of the present work is further improvement of reliability through the use of a panel of positive control compounds with well-characterized binding sites. Further, negative control compounds are also included to justify the selection threshold of the docking scores. The randomly chosen compounds with multiple aromatic rings demonstrate their role in the binding to the nucleobase pocket of NAMPT similar way as the substrate NAM. The docking poses of new candidate modulators predicted by CB-Dock2 are also compared with known modulators through 2-D protein-ligand interaction analysis to increase the confidence of the obtained results.

For validation purposes, known interactions of the active site of NAMPT with the substrate NAM through the Phe-193/Tyr-18 π−π clamp (with an Arg-311 edge interaction) were used (Tab. 1) [31]. Characterized NAMPT modulators (both activators and inhibitors) containing 4-pyridyl residues are known to bind to two locations within the active site of the enzyme, a nucleobase and “doorsill” orthosteric sites. The active doorsill site binds the substrate NAM and its analogs through amino acids (AA-s) Asp-219, Ser-241, Val-242, and Ser -275 (Tab. 1) [26]. The Asp-219 is important for the binding of NAM and His-247 is crucial for

autophosphorylation by ATP [38]. Positive allosteric NAMPT modulators N-PAMs do not, however, interact with the mentioned nucleobase pocket, but they are bound only to the "rear channel" [31] (Tab. 1). The large rear channel cavity is formed by Tyr-188/Gly-185/Ala-379 and Pro-272/Pro-307, with the tolyl group enclosed by His-191/Val-242/Ile-351 and the benzyl group by Arg-349/Val-350. In addition to the interaction with Lys-189, N-PAMs form a loose H-bonding network at the mouth of the rear channel including Thr-304 [26] (Tab. 1). These characterized interactions of NAMPT modulators with the active and allosteric sites will be applied for the validation of CB-Dock2 method and characterization of new NAMPT modulator candidates.

Here, the testing panel of 21 compounds was created, which included known NAMPT activators, inhibitors and control compounds (Tab. 2). As positive controls were used the substrate NAM; the product NMN; NAMPT activators NAT5-r [32], P7C3 (1-(3,6-dibromo-carbazol-9-yl)-3-phenylamino-propan-2-ol) [39], quercitrin [31], SBI-797812 [40], TIE (NP-A1-R; (3R)-1-[2-(4-methylphenyl)-2H-pyrazolo[3,4-d] pyrimidin-4-yl]-N-{[4-(methylsulfanyl)phenyl]methyl}piperidine-3-carboxamide) (PDB: 8DSC) [31], US11452717 (1-(4-((4-chlorophenyl)sulfonyl)phenyl)-3-(oxazol-5-ylmethyl)urea) [41], ZN-2-43 ((3S)-N-[(1-benzothiophen-5-yl)methyl]-1-{2-[4-(trifluoromethyl)phenyl]-2H-pyrazolo[3,4-d]pyrimidin-4-yl}piperidine-3-carboxamide) (PDB: 8TPJ) [31], and NAMPT inhibitors 1QR (N-[4-(piperidin-1-ylsulfonyl)benzyl]-1H-pyrrolo[3,2-c]pyridine-2-carboxamide) (PDB: 4KFN) [42], 20M (N-(4-{[4-(pyrrolidin-1-yl)piperidin-1-yl]sulfonyl}benzyl)-2H-pyrido[4,3-e][1,2,4]thiadiazin-3-amine 1,1-dioxide) (PDB: 4LVA; [43]), C5V ((1S,2S)-N-{4-[(1,3-dioxo-1,3-dihydro-2H-isoindol-2-yl)methyl]phenyl}-2-(pyridin-3-yl)cyclopropane-1-carboxamide) (PDB: 6AZJ), FK866 [44],

GMX1778 (2-[6-(4-chlorophenoxy)hexyl]-1-cyano-3-pyridin-4-ylguanidine) [45], GNE-617 and GNE-618 [46] [47] (Tab. 2).

CB-Dock2 validation was achieved by the inspection of NAM interactions with the active site of NAMPT by docking into 8DSI. The results displayed all three interactions with the key AA-s of the nucleobase pocket (Tyr-18, Phe-193, Asp-219; Tab. 1) (Fig. S1a). Further, N-PAM TIE (NP-A1-R) was anticipated to bind only to the doorsill and rear channel AA-s (Tab. 1) [31]. In agreement with these expectations, the molecular docking results did not display any strong π-π stacked and π-donor hydrogen bonds with Phe-193/Tyr-18 and hydrogen bond with Asp219, similar to the binding of the substrate NAM (Fig. S1a). The nucleobase pocket AA-s (Phe-193/Tyr-18) however, interacted with TIE by alkyl bonds, but not through π-bonds of aromatic rings as it occurs by interactions of NAM. The results also exhibited binding to the doorsill Val-242 and the rear channel Tyr-188, Ile-351, and Ala-379, which fits better with the previously reported results. VDW interactions with three additional AA-s involved in the doorsill site of NAMPT were also predicted here (Asp219, Ser241, Ser275) (Tab. 3; Fig. S1b).

Several known inhibitors and activators bind to the nucleobase pocket, as it was documented by docking of GNE-17, GNE-618, and ZN-2-43 (Fig. S1c-e). The CB-Dock2-predicted interactions confirmed previously reported strong π-π stacked interactions with the nucleobase pocket AA-s, which corresponds well to the high docking scores. The common feature of the known strong NAMPT inhibitors GNE-617 and GNE-618 is binding to the Phe-193/Tyr-18 π−π clamp [26]. The results of the molecular docking of GNE-617 into 8DSI (docking score -11,5 kcal/mol) showed strong π-π stacked and π-cation interactions with the nucleobase Phe-193 and Tyr-18 accompanied by π-cation and hydrogen interactions with the doorsill Asp-219 (Tab. 2; Tab. 3; Fig. S1c). GNE-618 when docked into 8DSC (docking score -12,5 kcal/mol) exhibited π-π

stacked interactions with Tyr-18/Phe-193 of the nucleobase pocket and hydrogen bonds with the doorsill Asp-219 and Phe-193 (Tab. 3; Fig. S1e).

NAMPT activator ZN-2-43 also exhibited high docking scores in the range from -10,7 to -12,7 kcal/mol with all studied crystal structures. Previously, the interactions with the nucleobase pocket of NAMPT were reported similar to interactions with NAM [31]. Here, a 2D diagram of the interaction with 4o13 (docking score -12,7 kcal/mol) confirmed π-π stacked interaction with Phe-193 and π-donor hydrogen bond with Tyr-18. Additional interactions were also visualized with AA-s of the doorsill and the rear channel (Tab. 2; Tab. 3; Fig. S1d).

The molecular docking scores of the potent activator NAT-5r (HY-148948) [21] did not reach the docking scores of the best candidate modulators (Tab. 2). However, when docked into 7ENQ ((NAMPT+NAT); the docking score -8,8), strong bonds with both the active and allosteric sites were predicted. Bonds with the nucleobase pocket were observed through π-π T-shaped and VDW interactions (Phe-193, Tyr-18). Further, π-alkyl (Val-242), hydrogen (Asp-219), and VDW interactions (Ser-241, Ser-275) of the doorsill and π-alkyl (Arg-349) and VDW interactions (Tyr-188, Lys, 189, His-191, Ala-379) of the rear channel were displayed (Tab. 3, Fig. S1f). Another potent inhibitor GMX1778 docked into the 8DSI structure exhibited interactions with Phe-193 by π-π stacked and alkyl bonds and with Tyr-18 by π−donor hydrogen bond (Tab. 3, Fig. S1g). Thus, GMX1778 showed identical nucleobase pocket interactions as the substrate NAM.

Negative controls (acetylsalicylsalicylic acid, maltose, melitriose, saccharose) were also used along with known positive control protein-ligand interactions (Tab. 2). They were chosen to match the new potential modulators of NAMPT by the molecular weight and water solubility. The docking of the random control compound acetylsalicylsalicylic acid into 4o13 (the docking score -8,7) (Tab. 2) exhibited the identical type of interactions as the substrate NAM (Tab. 3; Fig.

S2a), which occurs due to the presence of the aromatic rings. The docking scores, however, do not reach the values used as the threshold. The docking of maltose as a control compound without aromatic rings did not show any interactions with the key AA-s of the active and or allosteric site. CB-Dock2 predicted bonds with Arg-392 and Ser-398, which is similar to the binding of the NAMPT product NMN (data not shown) and melitriose (Tab. 3; Fig. S2b, c). The molecular docking of melitriose with M_r >500 g/mol showed only VDW interactions with Phe-193 and His-247. Additionally, when docked into 4o13 and 4N9C, the carbon-hydrogen bond with Phe-193 (data not shown) and hydrogen bond with Tyr-18 (4N9C) were detected (Fig. S2c). Mostly weak VDW accompanied by only single hydrogen interaction with the key AA-s of the nucleobase pocket and without the presence of π-interactions can be considered as a non-specific binding.

Eszopiclone was randomly chosen as a water-soluble control compound with a molecular weight in the studied range. Its chemical structure contains pyridine, pyrazine, piperidine, and pyrrole rings, therefore a strong interaction with the nucleobase pocket of NAMPT could be expected. Indeed, the aromatic benzene and pyridine rings exhibited similar interactions as NAM with the nucleobase AA-se through π-π stacked, π-donor hydrogen, and two alkyl bonds (Fig. S2d). However, no interactions were observed with the doorsill and the rear channel (Tab. 3; Fig. S2d). As a conclusion, 2D analysis of TIE interactions with the active and allosteric sites of NAMPT correlated well with the experimental results. The activator ZN-2-43 and strong inhibitors GNE-617, GNE-618, and GMX1778 exhibited interactions with the nucleobase pocket AA-s through π-π stacked, π-π T-shaped, and π−donor hydrogen bonds similar or identical to the binding of the substrate NAM. The molecular docking of these compounds was in good agreement with the experimental results. Multiple strong interactions of potent activator NAT-5r with the active and

allosteric sites of NAMPT showed however, the docking scores only around the threshold values and could be expected to be more negative. The analysis also concluded that the presence of the aromatic rings can increase the interactions with the nucleobase pocket similar to NAM. The saccharide types of ligands without aromatic rings tend to interact with AA residues similar to the product of NAMPT enzymatic activity NMN. The compounds with docking scores under the threshold value -9 kcal/mol predicted to interact with the nucleobase pocket by π-interactions and/or by multiple non-VDW interactions with the key doorsill and rear channel AA-s are with high probability true positive NAMPT modulators.

3. New potential modulators of NAMPT

It is considered a disadvantage that natural compounds have broad specificity since their effect is mediated by numerous protein targets. The definition of the mode of action of compounds originating from traditional medicinal plants is useful for the modulation of the target activities. Severe side effects often present when highly specific synthetic modulators are applied can be efficiently avoided using selected natural compounds with low toxicity.

The present virtual screening method yielded 17 compounds with better docking scores than some known NAMPT modulators (Tab. 2, Tab. S1). An overview of the selected compounds based on their chemical structure and their pharmacological parameters was constructed through the Cytoscape application Chemviz2 (Fig. 3; Tab. S2).

At the first stage of the analysis, the compounds with molecular docking scores higher than the threshold were examined by 2D protein-ligand analysis of their docking poses using the BIOVIA DSV tool (Fig. 2). Their protein-ligand interaction profiles were compared with known binding sites of characterized NAMPT activators and inhibitors and the candidate

NAMPT modulators were organized according to their interactions with the nucleobase pocket (Phe-193, Tyr-18) into three subgroups (Tab. 4). Andrographin, aurantiamide, isobavachromene, ononetin and sesamolin were predicted to interact strongest with the active site of NAMPT (Tab. 4, group I). Within this group, isobavachromene as the only candidate compound was predicted to interact with both the active and allosteric sites by stronger interactions than VDW bonds and it resulted in one of the lowest docking scores in the range from -9,4 to 11,8 kcal/mol (Tab. 2). Berberine, calcaratarin D, 14-deoxy-11,12-didehydroandrographolide, galanal A, isoandrographolide, pacovatinin A, pacovatinin C, and stylopine showed weak interactions with the nucleobase pocket through VDW interactions (Tab. 4, Group II) and hedychilactone A, hupehenine, isocoronarin D and pacovatinin B exhibited interactions only with the doorsill and the rear channel of NAMPT (Tab. 4, Group III).

Among new candidate modulators, flavone andrographin originating from *Andrographis paniculata* showed the docking score exceeding the threshold value -9 kcal/mol only when docked into co-crystallized structure 4o13 (NAMPT+GNE-618) (Tab. 2). Its interaction type is a strong nucleobase pocket binding with the weak doorsill and no rear channel binding (Tab. 4). It exhibited π-donor hydrogen and π-alkyl bond with Tyr-18; π-π stacked bond with Phe-193 and Van der Waals interactions with the doorsill Asp-219 and His-247 (Fig. 2a; Tab. S3).

The docking scores of the dipeptide aurantiamide had values in the range from -9,6 to -10,4 kcal/mol with the result of the binding profile with 4o13 similar to andrographin and NAM (Fig. 2b; Tab. 4, Tab S3). Aurantiamide is an exception on the compound list since it is poorly soluble in water (Tab. S1). This compound can be, however, quickly absorbed in rat tissues after oral administration and eliminated within 4 h without accumulation [48], which makes it

a good candidate for pharmacological purposes.

Another interesting natural compound is benzylisoquinoline berberine, which when docked into 8DSE showed weak interactions with nucleobase pocket by VDW bonds, strong bonds with the doorsill AA-s, and multiple interactions with the rear channel (Fig. 2c; Tab. 4, Tab. S3). Berberine is known to improve cognitive functions in animal models of AD [49] and its neuroprotective effects provide therapeutical possibilities for AD, PD, and HD treatments [50]. The molecular mechanism of its role in AD could involve the regulation of amyloid precursor protein (APP) processing to the β-amyloid. The oral administration of berberine to AD animal models, rabbits with brain injections of aluminium maltolate protected the hippocampus from neurodegeneration and decreased BACE1 activity [51]. It functions as a BACE1 inhibitor with IC50 > 100 μM [52], which was used as additional control by the docking into the structure 7MYI (score -9.7 kcal/mol). Potential neuroprotective effects could be mediated by the activation of NAMPT activity and boosting of the NAD^+/NADH ratio exposed by the present results.

The labdane diterpenoid calcaratarin D exhibited weak interactions with the nucleobase pocket through VDW bonds (Tab. 4). Stronger interactions with doorsill *via* hydrogen bonds (Ser-241, Val-242), carbon-hydrogen bond (Asp-219) and the rear channel by hydrogen (Tyr-188) and alkyl bonds (Arg-349, Ile-351, Ala-379) were also predicted (Fig. 2d; Tab. 4, Tab. S3). The interactions of another labdane diterpenoid 14-Deoxy-11,12-didehydroandrographolide included only weak VDW bonds with the nucleobase, doorsill, and rear channel AA-s. The exceptions were the hydrogen (Ser-241) and alkyl (Val-242) interactions at the doorsill (Fig. 2e; Tab. 4; Tab. S3) and they corresponded to the docking scores around the threshold values in the range from -8,4 to -9,5 kcal/mol (Tab. 2). Similarly, the diterpenoid galanal A also

exhibited weak VDW interactions with the nucleobase pocket, doorsill, and rear channel accompanied by only a few additional alkyl (Arg-349 and Ala-379), carbon-hydrogen (Tyr-188) and hydrogen (His-191) interactions within the rear channel (Fig. 2f; Tab. 4; Tab. S3). The docking poses also correlated well with the scores around the threshold values in the range from -8 to -9 kcal/mol (Tab. 2). Another labdane diterpenoid hedychilactone A did not exhibit any interaction with the nucleobase pocket of 8DSI (binding group III). It however, showed interactions with the doorsill through alkyl (Val-242) and VDW (Ser-241) bonds and with the rear channel by π-sigma (Tyr-188) and VDW interactions (His-191, Arg-349, Ala-379) (Fig. 2g; Tab. 4; Tab. S3). The alkaloid hupehenine also did not exhibit any binding to the nucleobase pocket, but it showed VDW interactions with the doorsill Ala-379 and alkyl bonds with the rear channel Arg-349, Ile-351, and (Fig. 2h; Tab. 4; Tab S3). Isoandrographolide, another member from the group of the labdane diterpenoids, exhibited weak VDW interaction with the nucleobase pocket (Phe-193), single hydrogen interaction with the doorsill (Ser-241), and interactions with the rear channel through the alkyl (Tyr-188) and hydrogen bonds (Lys-189). Additionally, multiple VDW interactions were predicted at both the doorsill and the allosteric site (Fig. 2i; Tab. 4, Tab. S3). These few predicted non-VDW interactions with the crucial AA-s also corresponded well to the docking scores around the threshold values in the range from -8,9 to -9,4 kcal/mol.

Flavone isobavachromene displayed binding to the nucleobase pocket the identical way as NAM when docked into 8DSE, 8DSI, 7ENQ, and 4o13 (Fig. 2j, Tab. S3). Additional interactions included hydrogen (Asp-219; Val-242) and VDW bonds with the doorsill, and alkyl (Ile-351) and multiple VDW interactions with the rear channel (Fig. 2j). It is the only compound among the candidate NAMPT modulators predicted to interact with both active and

allosteric sites by stronger bonds than VDW (Group I; Tab. 4). This finding correlates with high docking scores in the range from -9,4 to -11,8 kcal/mol (Tab. 2).

The labdane diterpenoid isocoronarin D belongs to the binding group III since no interaction was predicted with the nucleobase pocket. Further, it showed a weak VDW bond with the doorsill (Val-242) and hydrogen (Arg-349), alkyl (Ala-379), and multiple VDW interactions with the rear channel (Fig. 2k; Tab. 4, Tab. S3).

Ononetin is a stilbenoid originating from *Ononis spinosa* (Fabaceae), which is a part of traditional Russian medicine. Originally it was listed as a NAMPT activator in the work of Velma et al. (2024) [26], however, the experimental pieces of evidence are missing. Since the compound has low toxicity and is BBB-permeable, it was used for the molecular docking into NAMPT (Tab. 2). The binding type of group I was noticed when docked into 8DSI since the interaction with the nucleobase pocket and the doorsill was identical to the docking of NAM (Fig. 2l). The interactions with the doorsill Asp-219 and His-247 were observed through hydrogen bonds (Fig. 2l; Tab. 4; Tab. S3).

Labdane terpenoids pacovatinin A-C interacted weakly or not at all with AA-s of the nucleobase pocket and the doorsill AA. Only a few additional interactions with the rear channel of the type π-sigma, alkyl, and hydrogen bonds were predicted, which suggests the modulation of NAMPT activity mostly through the allosteric site (Tab. 4). Pacovatinin A docked into 8DSE displayed weak VDW interactions with AA-s of the active and allosteric sites. Additional alkyl interactions with Arg-349; and Ala-375 located at the rear channel were displayed as well (Fig. 2m; Tab. 4; Tab. S3). Pacovatinin B showed the highest molecular docking score -9,4 kcal/mol when docked into 7ENQ (NAMPT+NAT). It exhibited only weak VDW with the doorsill (Ser-241, Val-242) and rear channel (Lys-189; His-191; Arg-349, Ala-

379), accompanied by only one π-sigma interaction with the rear channel (Tyr-188) AA-s (Fig. 2n; Tab. 4; Tab. S3). Highest docking score of pacovatinin C was achieved with 7ENQ (NAMPT+NAT) and it also corresponded mostly to VDW interactions with AA-s of the nucleobase (Phe-193), the doorsill (Val-242, Ser-275) and the rear channel (Tyr-188, Lys-189, Ile-351 and Ala-379). Additional hydrogen bonds with the rear channel (His-191 and Arg-349) were also observed (Fig. 2o; Tab. 4; Tab. S3). Overall, the interactions of pacovatinin A-C with the protein crystal structures of NAMPT were weak and on the borderline of true interactions. Their chemical structures do not contain any aromatic rings interacting strongly with the nucleobase pocket (Tab. S2). The predicted interactions with the doorsill and rear channel AA-s appear however, more specific compared to the negative controls (Fig. 2m-o; Tab. 4; Tab. S3), and therefore, they are still included in the list of the selected candidate modulators.

The most negative molecular docking scores in the range from -10,3 to -11,8 were obtained for the dioxole sesamolin. When docked into 8DSI (NAMPT+NAM), sesamolin displayed the same type of bonds with the nucleobase pocket and the doorsill as the substrate NAM (Fig. 2p; Group I; Tab. 4 and Tab. S3). The observation correlates well with the docking scores and the presence of two aromatic rings in the chemical structure (Tab. S2). The benzylisoquinoline stylopine also showed high scores by docking into all NAMPT co-crystallized structures. When docked into the 7ENQ (score -11,2 kcal/mol), the interaction with the nucleobase pocket was displayed only through VDW interaction with Phe-193. Further, it showed interactions with the doorsill by π-alkyl (Val-242), hydrogen (Ser-275), and VDW (Ser-241) bonds. The rear channel interactions included π-alkyl (Arg-349, Ile-351), π-sigma (Ala-379) and VDW (His-191, Tyr-188) bonds (Fig. 2r; Group II; Tab. 4; Tab. S3).

The comparison of the compound binding to the key AA-s of the nucleobase pocket, doorsill,

and the rear channel did not show any significant difference between the known and selected candidate modulators. As a general observation during the screening candidate NAMPT modulators, the occurrence of π-π stacked, π-sigma, π-alkyl, and π-donor hydrogen bonds with the corresponding AA-s of the active (nucleobase and doorsill) and allosteric site (rear channel) correlated with more negative docking scores. The incidence of predominantly Van der Waals interactions with only a few additional types of interactions with the crucial AA-s corresponded to the docking scores around the threshold value -9 kcal/mol.

Since the natural modulators have multiple targets, they should perform finer tuning of NAMPT activity by their oral administration. The reason to avoid a robust increase of NAMPT activity is the subsequent activation of NAD^+-dependent enzymes SIRT-s and PARP-s with boosting of their diverse functions. Both NAMPT activity decline and excessive increase have a negative impact on pressure overload-induced heart failure. This example of the negative effect of the high NAD^+ production boosting demonstrates the negative impacts on organs such as the heart [53]. All members of the SIRT family perform important tasks in the heart functions and excessive dysregulation of their activities can also have negative effects. Extreme increase in SIRT-s activity is detrimental to cardiomyocytes, which can be prevented by boosting NAMPT-dependent NAD^+ production by NAM, an inhibitor of SIRT-s [53]. This strategy would not, however, function in the brain, since NAM is not able to pass BBB.

The overexpression of NAMPT also had an undesirable effect in $APOE^{-/-}$ mice, a model of atherosclerosis, where NAMPT promoted atherosclerotic inflammation [54]. These examples, however, illustrate effects due to extreme even multiple times changes of NAMPT expression and they are the results from models with severe dysregulations. The increasing of NAMPT activity in small increments should be a choice and the natural compounds can provide such

alternatives. The development of NAMPT inhibitors for cancer treatment also failed multiple times, because of the ability of cancer cells to produce NAD^+ by alternative pathways [26]. Progress in the development of NAMPT inhibitors should be achieved by the identification of the tumor types based on NAD^+ production pathways as a part of the precision medicine strategy.

4. Conclusions

The present study used a virtual screening method for the identification of candidate modulators of NAMPT activity. The computer-based selection method offers a low-cost alternative to experimental screening, the final evaluation must, however, be always performed by laboratory experimentation.

NAMPT activators are desired for the enhancement of mitochondrial bioenergetics during normal aging and/or for the improvement of conditions of patients with neurodegenerative diseases such as AD, PD, and HD through boosting the cellular NAD^+/NADH ratio. Increasing NAD^+ production could also provide aging-related benefits by stimulating the activity of NAD^+-dependent SIRT-s; however, small stimulatory increments should be chosen because of possible negative effects. Potential NAMPT inhibitors could be used for the limitation of the cancer cell growth if the tumor type is dependent on the salvage pathway of NAD^+ production, which should be determined by the precision medicine approach. Here, the advantage is that the selected compounds do not contribute to additional toxicity to the normal cells.

Pre-screening 231 compounds originating from traditional African, Chinese, and Russian medicinal plants resulted in the selection of 17 compounds. These compounds with low toxicity should be able to pass BBB and they fulfill basic pharmacological criteria. They are predicted to interact with the active and/or allosteric sites of NAMPT through specific AA residues similar to

characterized NAMPT activators and inhibitors. The selected potential modulators of NAMPT activity could be used as an initial point for the development of therapeutical applications.

Declarations and statements

Acknowledgments

The research was conducted from the financial resources of Biochemworld Co., Uppsala County, Sweden.

Data availability

All generated data are available as figures, tables, and supplementary material excluding the list of the plant compounds used for the virtual screening. The information can be provided by the corresponding author upon the request.

Competing interests

The author is a founder of a non-profit organization Biochemworld Co.

CRediT author statement

Jarmila Nahálková: Artwork, Conceptualization, Correspondence, Data curation, Formal analysis, Funding acquisition, Investigation, Methodology, Project administration, Resources, Software, Validation, Visualization, Writing - original draft, Writing - review & editing

Declaration of generative AI and AI-assisted technologies in the writing process

No AI-assisted technologies were used in the present manuscript neither for figures nor manuscript text generation.

5. References

[1] D. Nicholls, Mitochondrial bioenergetics, aging, and aging-related disease, Sci. Aging Knowl. Environ. 2002 (2002) pe12–pe12. https://doi.org/10.1126/sageke.2002.31.pe12.

[2] S. Lautrup, D.A. Sinclair, M.P. Mattson, E.F. Fang, NAD+ in brain aging and neurodegenerative disorders, Cell Metab. 30 (2019) 630–655. https://doi.org/10.1016/j.cmet.2019.09.001.

[3] S. Lehmann, S.H.Y. Loh, L.M. Martins, Enhancing NAD+ salvage metabolism is neuroprotective in a PINK1 model of Parkinson's disease, Biol. Open. 6 (2016) 141–147. https://doi.org/10.1242/bio.022186.

[4] M.P. Mattson, T. V. Arumugam, Hallmarks of brain aging: Adaptive and pathological modification by metabolic states, Cell Metab. 27 (2018) 1176–1199. https://doi.org/10.1016/j.cmet.2018.05.011.

[5] A. Garten, S. Petzold, A. Körner, S. Imai, W. Kiess, Nampt: Linking NAD biology, metabolism, and cancer, Trends Endocrinol. Metab. 20 (2009) 130.

[6] M. Emanuelli, F. Carnevali, F. Saccucci, F. Pierella, A. Amici, N. Raffaelli, G. Magni,

Molecular cloning, chromosomal localization, tissue mRNA levels, bacterial expression, and enzymatic properties of human NMN adenylyltransferase, J. Biol. Chem. 276 (2001) 406–412. https://doi.org/10.1074/jbc.M008700200.

[7] M. Schweiger, K. Hennig, F. Lerner, M. Niere, M. Hirsch-Kauffmann, T. Specht, C. Weise, S.L. Oei, M. Ziegler, Characterization of recombinant human nicotinamide mononucleotide adenylyl transferase (NMNAT), a nuclear enzyme essential for NAD synthesis, FEBS Lett. 492 (2001) 95–100. https://doi.org/10.1016/s0014-5793(01)02180-9.

[8] J.R. Revollo, A.A. Grimm, S.I. Imai, The NAD biosynthesis pathway mediated by nicotinamide phosphoribosyltransferase regulates Sir2 activity in mammalian cells, J. Biol. Chem. 279 (2004) 50754–50763. https://doi.org/10.1074/jbc.M408388200.

[9] M. Yoshida, A. Satoh, J.B. Lin, K.F. Mills, Y. Sasaki, N. Rensing, M. Wong, R.S. Apte, S.-I. Imai, Extracellular vesicle-contained eNAMPT delays aging and extends lifespan in mice, Cell Metab. 30 (2019) 329-342.e5. https://doi.org/10.1016/j.cmet.2019.05.015.

[10] X. Wang, Q. Zhang, R. Bao, N. Zhang, Y. Wang, L. Polo-Parada, A. Tarim, A. Alemifar, X. Han, H.M. Wilkins, Deletion of Nampt in projection neurons of adult mice leads to motor dysfunction, Neurodegeneration, and Death, Cell Rep. 20 (2017) 2184–2200.

[11] C. Chen, T. Wang, T.-Y. Gao, Y.-L. Chen, Y.-B. Lu, W.-P. Zhang, Ablation of NAMPT in dopaminergic neurons leads to neurodegeneration and induces Parkinson’s disease in mouse, Brain Res. Bull. 218 (2024) 111114. https://doi.org/https://doi.org/10.1016/j.brainresbull.2024.111114.

[12] J.R. Revollo, A. Körner, K.F. Mills, A. Satoh, T. Wang, A. Garten, B. Dasgupta, Y.

Sasaki, C. Wolberger, R.R. Townsend, J. Milbrandt, W. Kiess, S.-I. Imai, Nampt/PBEF/Visfatin regulates insulin secretion in beta cells as a systemic NAD biosynthetic enzyme, Cell Metab. 6 (2007) 363–375. https://doi.org/10.1016/j.cmet.2007.09.003.

[13] E.F. Fang, Y. Hou, K. Palikaras, B.A. Adriaanse, Mitophagy inhibits amyloid-β and tau pathology and reverses cognitive deficits in models of Alzheimer's disease, Nat Neurosci. 22 (2019) 401–412.

[14] M.P. Mattson, M. Gleichmann, A. Cheng, Mitochondria in neuroplasticity and neurological Disorders, Neuron. 60 (2008) 748–766. https://doi.org/10.1016/j.neuron.2008.10.010.

[15] E.F. Fang, Mitophagy and NAD+ inhibit Alzheimer disease., Autophagy. 15 (2019) 1112–1114.

[16] W. Qin, T. Yang, L. Ho, Z. Zhao, J. Wang, L. Chen, W. Zhao, M. Thiyagarajan, D. MacGrogan, J.T. Rodgers, P. Puigserver, J. Sadoshima, H. Deng, S. Pedrini, S. Gandy, A.A. Sauve, G.M. Pasinetti, Neuronal SIRT1 activation as a novel mechanism underlying the prevention of Alzheimer disease amyloid neuropathology by calorie restriction, J. Biol. Chem. 281 (2006) 21745–21754. https://doi.org/10.1074/jbc.M602909200.

[17] Y. Sasaki, T. Araki, J. Milbrandt, Stimulation of Nicotinamide Adenine Dinucleotide biosynthetic pathways delays axonal degeneration after axotomy, J. Neurosci. 26 (2006) 8484–8491.

[18] C. Canto, R.H. Houtkooper, E. Pirinen, D.Y. Youn, M.H. Oosterveer, Y. Cen, P.J. Fernandez-Marcos, H. Yamamoto, P.A. Andreux, P. Cettour-Rose, The NAD precursor

nicotinamide riboside enhances oxidative metabolism and protects against high-fat diet-induced obesity, Cell Metab. 15 (2012) 838–847.

[19] A.N. Long, K. Owens, A.E. Schlappal, T. Kristian, P.S. Fishman, R.A. Schuh, Effect of nicotinamide mononucleotide on brain mitochondrial respiratory deficits in an Alzheimer's disease-relevant murine model, BMC Neurol. 15 (2015) 1–14. https://doi.org/10.1186/s12883-015-0272-x.

[20] S. Xing, Y. Hu, X. Huang, D. Shen, C. Chen, Nicotinamide phosphoribosyltransferase□related signaling pathway in early Alzheimer's disease mouse models, Mol. Med. Rep. 20 (2019) 5163–5171. https://doi.org/10.3892/mmr.2019.10782.

[21] B. Tan, D.A. Young, Z.-H. Lu, T. Wang, T.I. Meier, R.L. Shepard, K. Roth, Y. Zhai, K. Huss, M.-S. Kuo, Pharmacological inhibition of nicotinamide phosphoribosyltransferase (NAMPT), an enzyme essential for NAD+ biosynthesis, in human cancer cells: metabolic basis and potential clinical implications, J. Biol. Chem. 288 (2013) 3500–3511.

[22] F. Ntie-Kang, P.A. Onguéné, G.W. Fotso, K. Andrae-Marobela, M. Bezabih, J.C. Ndom, B.T. Ngadjui, A.O. Ogundaini, B.M. Abegaz, L.M. Meváa, Virtualizing the p-ANAPL library: A step towards drug discovery from African medicinal plants, PLoS One. 9 (2014). https://doi.org/10.1371/journal.pone.0090655.

[23] D. Zofou, F. Ntie-Kang, W. Sippl, S.M.N. Efange, Bioactive natural products derived from the Central African flora against neglected tropical diseases and HIV, Nat. Prod. Rep. 30 (2013) 1098–1120. https://doi.org/10.1039/c3np70030e.

[24] A.K. Gupta, A. Jain, Phyto-chemical and therapeutic briefing of Kigelia africana (Lam.) Benth, Indian J. Pharm. Biol. Res. 7 (2019) 14–22. https://doi.org/10.30750/ijpbr.7.1.4.

[25] J. Gan, J. Liu, Y. Liu, S. Chen, W. Dai, Z.-X. Xiao, Y. Cao, DrugRep: an automatic virtual screening server for drug repurposing, Acta Pharmacol. Sin. 44 (2023) 888–896. https://doi.org/10.1038/s41401-022-00996-2.

[26] G.R. Velma, I.S. Krider, E.T.M. Alves, J.M. Courey, M.S. Laham, G.R.J. Thatcher, Channeling Nicotinamide Phosphoribosyltransferase (NAMPT) to Address Life and Death, J. Med. Chem. 67 (2024) 5999–6026. https://doi.org/10.1021/acs.jmedchem.3c02112.

[27] A. Daina, O. Michielin, V. Zoete, SwissADME: a free web tool to evaluate pharmacokinetics, drug-likeness and medicinal chemistry friendliness of small molecules, Sci. Rep. 7 (2017) 42717. https://doi.org/10.1038/srep42717.

[28] P. Banerjee, A.O. Eckert, A.K. Schrey, R. Preissner, ProTox-II: a webserver for the prediction of toxicity of chemicals, Nucleic Acids Res. 46 (2018) W257–W263. https://doi.org/10.1093/nar/gky318.

[29] Y. Liu, X. Yang, J. Gan, S. Chen, Z.X. Xiao, Y. Cao, CB-Dock2: improved protein-ligand blind docking by integrating cavity detection, docking and homologous template fitting, Nucleic Acids Res. 50 (2022) W159–W164. https://doi.org/10.1093/nar/gkac394.

[30] Protein Data Bank: the single global archive for 3D macromolecular structure data, Nucleic Acids Res. 47 (2019) D520–D528. https://doi.org/10.1093/nar/gky949.

[31] K.M. Ratia, Z. Shen, J. Gordon-Blake, H. Lee, M.S. Laham, I.S. Krider, N. Christie, M. Ackerman-Berrier, C. Penton, N.G. Knowles, S.R. Musku, J. Fu, G.R. Velma, R. Xiong, G.R.J.J. Thatcher, Mechanism of allosteric modulation of Nicotinamide Phosphoribosyltransferase to elevate cellular NAD+, Biochemistry. 62 (2023) 923–933.

https://doi.org/10.1021/acs.biochem.2c00655.

[32] H. Yao, M. Liu, L. Wang, Y. Zu, C. Wu, C. Li, R. Zhang, H. Lu, F. Li, S. Xi, S. Chen, X. Gu, T. Liu, J. Cai, S. Wang, M. Yang, G.-G. Xing, W. Xiong, L. Hua, Y. Tang, G. Wang, Discovery of small-molecule activators of nicotinamide phosphoribosyltransferase (NAMPT) and their preclinical neuroprotective activity, Cell Res. 32 (2022) 570–584. https://doi.org/10.1038/s41422-022-00651-9.

[33] W. Wang, K. Elkins, A. Oh, Y.-C. Ho, J. Wu, H. Li, Y. Xiao, M. Kwong, M. Coons, B. Brillantes, E. Cheng, L. Crocker, P.S. Dragovich, D. Sampath, X. Zheng, K.W. Bair, T. O'Brien, L.D. Belmont, Structural basis for resistance to diverse classes of NAMPT inhibitors, PLoS One. 9 (2014) e109366. https://doi.org/10.1371/journal.pone.0109366.

[34] P.S. Dragovich, G. Zhao, T. Baumeister, B. Bravo, A.M. Giannetti, Y.-C. Ho, R. Hua, G. Li, X. Liang, X. Ma, T. O'Brien, A. Oh, N.J. Skelton, C. Wang, W. Wang, Y. Wang, Y. Xiao, P. Yuen, M. Zak, Q. Zhao, X. Zheng, Fragment-based design of 3-aminopyridine-derived amides as potent inhibitors of human nicotinamide phosphoribosyltransferase (NAMPT), Bioorg. Med. Chem. Lett. 24 (2014) 954–962. https://doi.org/10.1016/j.bmcl.2013.12.062.

[35] C.T. Lopes, M. Franz, F. Kazi, S.L. Donaldson, Q. Morris, G.D. Bader, Cytoscape Web: an interactive web-based network browser, Bioinformatics. 26 (2010) 2347–2348. https://doi.org/10.1093/bioinformatics/btq430.

[36] J.D. Morris J, ChemViz2: Cheminformatics app for Cytoscape, (2015). http://www.cgl.ucsf.edu/cytoscape/chemViz2/index.shtml (accessed June 26, 2024).

[37] M. García-Ortegón, G.N.C. Simm, A.J. Tripp, J.M. Hernández-Lobato, A. Bender, S.

Bacallado, Dockstring: Easy molecular docking yields better benchmarks for ligand design, J. Chem. Inf. Model. 62 (2022) 3486–3502. https://doi.org/10.1021/acs.jcim.1c01334.

[38] D. Houry, A. Raasakka, E. Ferrario, M. Niere, E. Bifulco, P. Kursula, M. Ziegler, Identification of structural determinants of nicotinamide phosphoribosyl transferase (NAMPT) activity and substrate selectivity, J. Struct. Biol. 215 (2023) 108004. https://doi.org/10.1016/j.jsb.2023.108004.

[39] G. Wang, T. Han, D. Nijhawan, P. Theodoropoulos, J. Naidoo, S. Yadavalli, H. Mirzaei, A.A. Pieper, J.M. Ready, S.L. McKnight, P7C3 neuroprotective chemicals function by activating the rate-limiting enzyme in NAD salvage, Cell. 158 (2014) 1324–1334. https://doi.org/10.1016/j.cell.2014.07.040.

[40] S.J. Gardell, M. Hopf, A. Khan, M. Dispagna, E. Hampton Sessions, R. Falter, N. Kapoor, J. Brooks, J. Culver, C. Petucci, C.-T. Ma, S.E. Cohen, J. Tanaka, E.S. Burgos, J.S. Hirschi, S.R. Smith, E. Sergienko, A.B. Pinkerton, Boosting NAD+ with a small molecule that activates NAMPT, Nat. Commun. 10 (2019) 3241. https://doi.org/10.1038/s41467-019-11078-z.

[41] A.B. Pinkerton, E.H. Sessions, P. Hershberger, P.R. Maloney, S. Peddibhotla, M. Hopf, E. Sergienko, C.-T. Ma, L.H. Smith, M.R. Jackson, J. Tanaka, T. Tsuji, M. Akiu, S.E. Cohen, T. Nakamura, S.J. Gardell, Optimization of a urea-containing series of nicotinamide phosphoribosyltransferase (NAMPT) activators, Bioorg. Med. Chem. Lett. 41 (2021) 128007. https://doi.org/https://doi.org/10.1016/j.bmcl.2021.128007.

[42] X. Zheng, P. Bauer, T. Baumeister, A.J. Buckmelter, M. Caligiuri, K.H. Clodfelter, B.

Han, Y.-C. Ho, N. Kley, J. Lin, D.J. Reynolds, G. Sharma, C.C. Smith, Z. Wang, P.S. Dragovich, A. Oh, W. Wang, M. Zak, J. Gunzner-Toste, G. Zhao, P. Yuen, K.W. Bair, Structure-based identification of ureas as novel nicotinamide phosphoribosyltransferase (Nampt) inhibitors, J. Med. Chem. 56 (2013) 4921–4937. https://doi.org/10.1021/jm400186h.

[43] X. Zheng, K.W. Bair, P. Bauer, T. Baumeister, K.K. Bowman, A.J. Buckmelter, M. Caligiuri, K.H. Clodfelter, Y. Feng, B. Han, Y.-C. Ho, N. Kley, H. Li, X. Liang, B.M. Liederer, J. Lin, J. Ly, T. O'Brien, J. Oeh, A. Oh, D.J. Reynolds, D. Sampath, G. Sharma, N. Skelton, C.C. Smith, J. Tremayne, L. Wang, W. Wang, Z. Wang, H. Wu, J. Wu, Y. Xiao, G. Yang, P. Yuen, M. Zak, P.S. Dragovich, Identification of amides derived from 1H-pyrazolo[3,4-b]pyridine-5-carboxylic acid as potent inhibitors of human nicotinamide phosphoribosyltransferase (NAMPT), Bioorg. Med. Chem. Lett. 23 (2013) 5488–5497. https://doi.org/10.1016/j.bmcl.2013.08.074.

[44] M. Hasmann, I. Schemainda, FK866, a highly specific noncompetitive inhibitor of nicotinamide phosphoribosyltransferase, represents a novel mechanism for induction of tumor cell apoptosis, Cancer Res. 63 (2003) 7436–7442.

[45] M. Watson, A. Roulston, L. Bélec, X. Billot, R. Marcellus, D. Bédard, C. Bernier, S. Branchaud, H. Chan, K. Dairi, K. Gilbert, D. Goulet, M.-O. Gratton, H. Isakau, A. Jang, A. Khadir, E. Koch, M. Lavoie, M. Lawless, M. Nguyen, D. Paquette, É. Turcotte, A. Berger, M. Mitchell, G.C. Shore, P. Beauparlant, The small molecule GMX1778 is a potent inhibitor of NAD+ biosynthesis: Strategy for enhanced therapy in nicotinic acid phosphoribosyltransferase 1-deficient tumors, Mol. Cell. Biol. 29 (2009) 5872–5888. https://doi.org/10.1128/MCB.00112-09.

[46] T. O'Brien, J. Oeh, Y. Xiao, X. Liang, A. Vanderbilt, A. Qin, L. Yang, L.B. Lee, J. Ly, E. Cosino, J.A. LaCap, A. Ogasawara, S. Williams, M. Nannini, B.M. Liederer, P. Jackson, P.S. Dragovich, D. Sampath, Supplementation of nicotinic acid with NAMPT inhibitors results in loss of in vivo efficacy in NAPRT1-deficient tumor models, Neoplasia (United States). 15 (2013) 1314–1329. https://doi.org/10.1593/neo.131718.

[47] Y. Xiao, K. Elkins, J.K. Durieux, L. Lee, J. Oeh, L.X. Yang, X. Liang, C. DelNagro, J. Tremayne, M. Kwong, B.M. Liederer, P.K. Jackson, L.D. Belmont, D. Sampath, T. O'Brien, Dependence of tumor cell lines and patient-derived tumors on the NAD salvage pathway renders them sensitive to NAMPT inhibition with GNE-618, Neoplasia. 15 (2013) 1151–1160. https://doi.org/10.1593/neo.131304.

[48] L. Chen, Y. Liu, D. Jia, J. Yang, J. Zhao, C. Chen, H. Liu, X. Liang, Pharmacokinetics and biodistribution of aurantiamide and aurantiamide acetate in rats after oral administration of Portulaca oleracea L. extracts, J. Agric. Food Chem. 64 (2016) 3445–3455. https://doi.org/10.1021/acs.jafc.6b00470.

[49] J.Y. Liu, Y. Dai, Y.X. He, L. Lin, Effect of berberine on cognitive function and β-amyloid precursor protein in Alzheimer's disease models: a systematic review and meta-analysis, Front. Pharmacol. 14 (2023) 1–14. https://doi.org/10.3389/fphar.2023.1301102.

[50] Z. Cai, C. Wang, W. Yang, Role of berberine in Alzheimer's disease, Neuropsychiatr. Dis. Treat. 12 (2016) 2509–2520. https://doi.org/10.2147/NDT.S114846.

[51] N. Panahi, M. Mahmoudian, P. Mortazavi, G.S. Hashjin, Effects of berberine on β-secretase activity in a rabbit model of Alzheimer's disease, Arch. Med. Sci. 9 (2013) 146–150. https://doi.org/10.5114/aoms.2013.33354.

[52] H.A. Jung, B.-S. Min, T. Yokozawa, J.-H. Lee, Y.S. Kim, J.S. Choi, Anti-Alzheimer and antioxidant activities of Coptidis Rhizoma alkaloids, Biol. Pharm. Bull. 32 (2009) 1433–1438.

[53] J. Byun, S. Oka, N. Imai, C.-Y. Huang, G. Ralda, P. Zhai, Y. Ikeda, S. Ikeda, J. Sadoshima, Both gain and loss of Nampt function promote pressure overload-induced heart failure, Am. J. Physiol. Circ. Physiol. 317 (2019) H711–H725. https://doi.org/10.1152/ajpheart.00222.2019.

[54] Y. Kong, G. Li, W. Zhang, X. Hua, C. Zhou, T. Xu, Z. Li, P. Wang, C. Miao, Nicotinamide phosphoribosyltransferase aggravates inflammation and promotes atherosclerosis in ApoE knockout mice, Acta Pharmacol. Sin. 40 (2019) 1184–1192. https://doi.org/10.1038/s41401-018-0207-3.

Fig. 1 Workflow of the virtual NAMPT modulator screening originated from traditional African, Chinese, and Russian medicinal plants. (1) Firstly, 231 compounds were collected from the libraries of African medicinal plants, DrugRep screening (Chinese traditional medicine), and Russian traditional medicine (ononetin). (2) The compounds were pre-screened by Swiss ADME and Pro-Tox II for BBB permeability, the best predicted pharmacological properties, and low toxicity. Pre-screened compounds were further subjected to molecular docking by CB-Dock2. (3) 2D protein-ligand analysis of the selected and control compounds was performed for validation of the docking method and the comparison of their interactions

Fig. 2 2D diagrams of the protein-ligand interactions between the selected compounds and the key amino acids of the nucleobase pocket, doorsill, and rear channel. The interactions are visualized by BIOVIA Discovery Studio Visualizer after molecular docking of the compounds with the protein crystal structures of NAMPT employing the molecular docking tool CB-Dock2

Fig. 3 The network of the selected 17 plant compounds constructed by importing the list containing chemical names and smile identifiers to the cheminformatics application ChemViz2 allowing the construction of the chemical structure similarity network. The results are presented after the Prefuse force-directed layout, where the node distance and the number of common links define the structural similarity in a fingerprint-like manner

Tab. 1 An overview of the key amino acids of the active and allosteric sites of NAMPT involved in the binding of known modulators

Tab. 2 Molecular docking scores of the selected candidate NAMPT modulators and control compounds using the tool CB-Dock2. Protein crystal structures: 8DSC (NAMPT+NAM+co-activator NP-A1-R); 7ENQ (NAMPT+activator NAT); 8DSE (NAMPT+NAM+activator quercitrin); 8DSI (NAMPT+NAM); 4o13 (NAMPT+inhibitor GNE-618); 4N9C (NAMPT+inhibitor 5-nitro-1H-benzimidazole)

Tab. 3 The types of the bonds involved in the protein-ligand interactions of positive, negative, and randomly chosen control compounds with the active and allosteric sites of NAMPT

Tab. 4 The types of the bonds involved in the protein-ligand interactions of 17 selected candidate NAMPT modulators with the active and allosteric sites of NAMPT

Fig. S1 2D diagrams of the protein-ligand interactions between the positive control compounds and the key amino acids of the nucleobase pocket, doorsill, and rear channel. The interactions were visualized by BIOVIA Discovery Studio Visualizer after molecular docking of the compounds with the protein crystal structures of NAMPT using the docking tool CB-Dock2

Fig. S2 The 2D diagrams of the protein-ligand interactions between the negative and randomly chosen control compounds and the key nucleobase pocket, doorsill, and rear channel amino acids. The interactions were visualized by BIOVIA Discovery Studio Visualizer after molecular docking of the compounds with the protein crystal structures of NAMPT using the docking tool CB-Dock2

Tab. S1 Overview of the selected candidate NAMPT modulators including their pharmacological characteristics predicted by SwissADME and ProTox-II

Tab. S2 Pharmacological parameters of 17 selected candidate NAMPT modulators exported from cheminformatics application Chemviz2 run under the Cytoscape 3.10.2 environment

Tab. S3 The types of the bonds involved in the protein-ligand interactions of 17 selected candidate NAMPT modulators with the specific key amino acids of the active and allosteric sites of NAMPT

Libraries of African medicinal plants

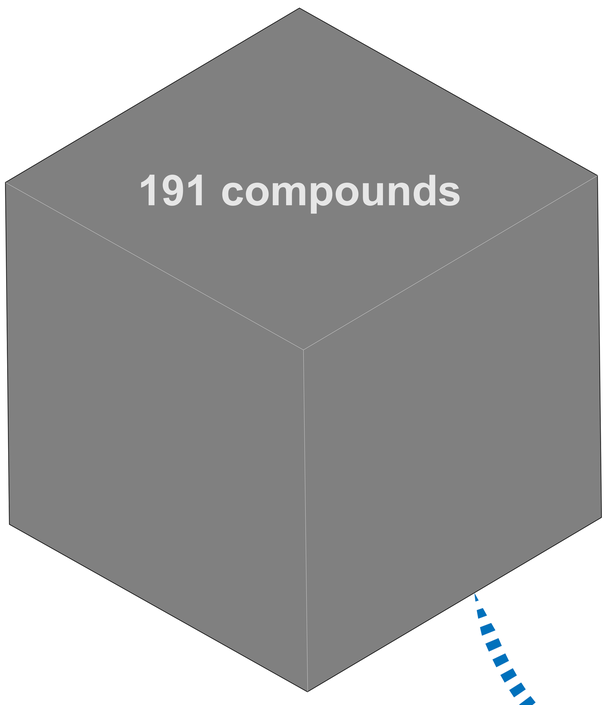

- Compounds from African medicinal plants
- P-ANAPL library
- Bioactive compounds from central African flora
- Phytochemicals from *Kigelia africana*

DrugRep libraries

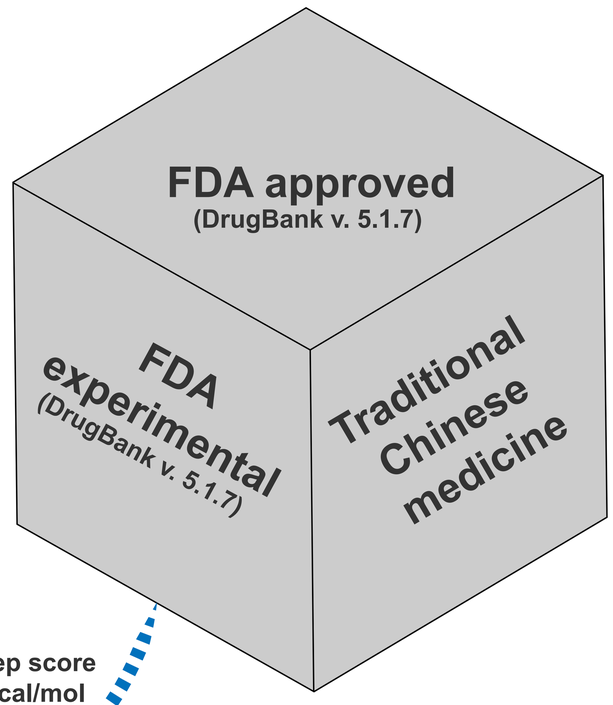

DrugRep score
> -9 kcal/mol

- DrugBank (version 5.1.7)
  > 500 000 compounds
- Traditional Chinese medicine library
  (2390 compounds
  from 800 traditional medicines)
- Receptor-based search
  (8DSI, 8DSE, 8DSC, 7ENQ)

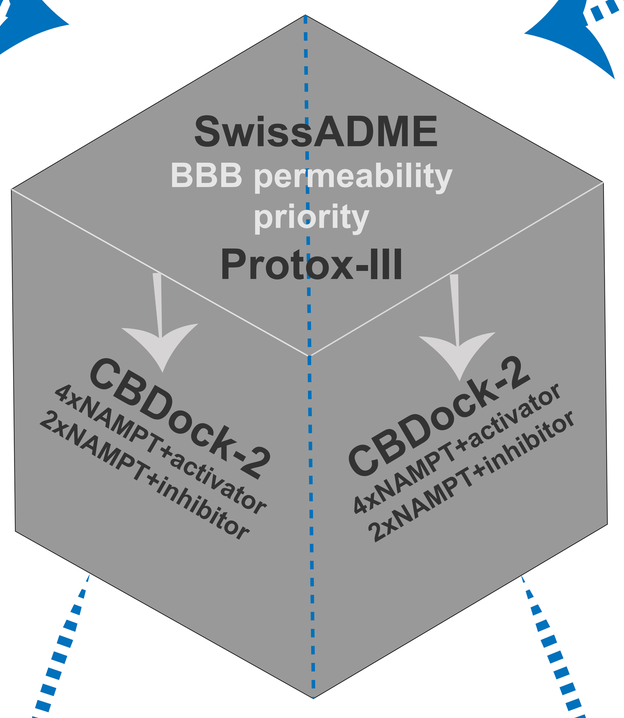

- score >-9kcal/mol
- BBB permeable
- High GI absorption
- Max 1 Lipinski´s rule violation
- Medium-high water solubility
- Low toxicity

2D protein-ligand interaction analysis

CBDock-2 validation and screening of new NAMPT modulators

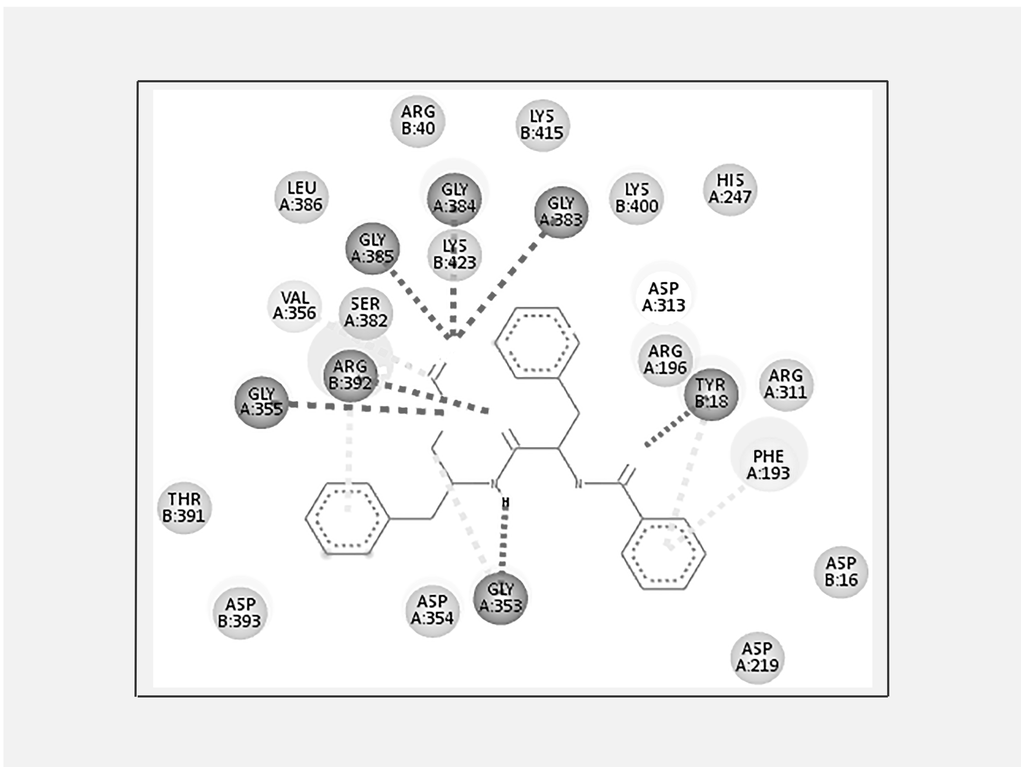

17 candidate NAMPT modulators
(activators or inhibitors)

4o13+andrographin

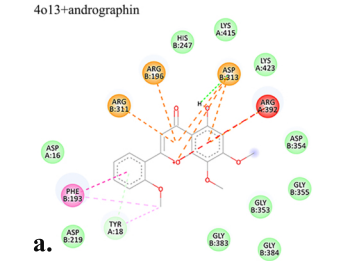

a.

4o13+aurantiamide

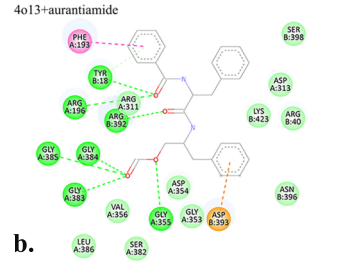

b.

8DSE+berberine

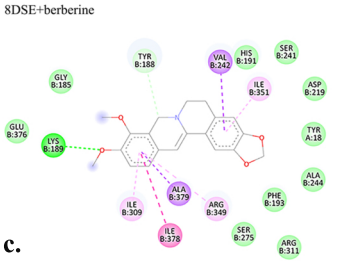

c.

8DSI+calcaratarin D

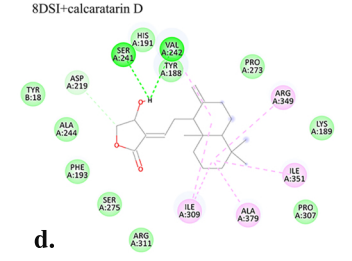

d.

4N9C+14-Deoxy-11,12-didehydroandrographolide

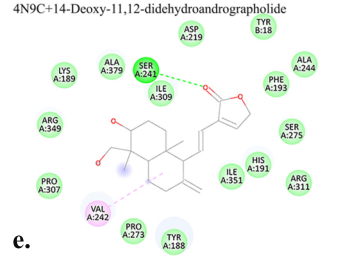

e.

7ENQ+galanal A

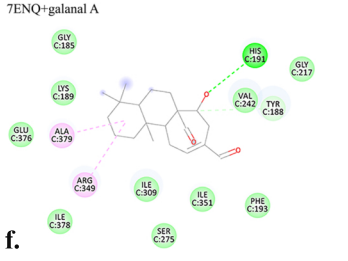

f.

8DSI+hedychilactone A

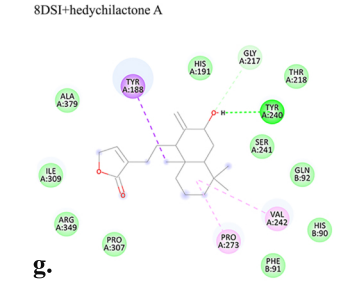

g.

7ENQ+hupehenine

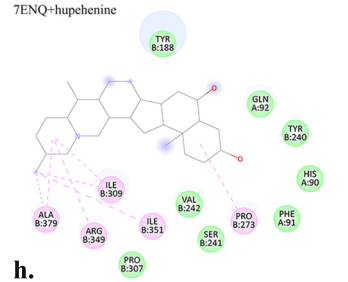

h.

7ENQ+isoandrographolide

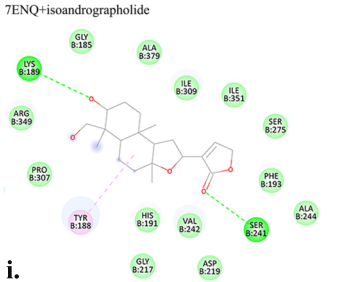

i.

8DSE+isobavachromene

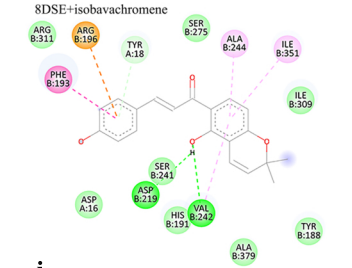

j.

8DSC+isocoronarin D

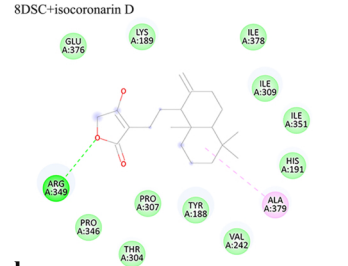

k.

8DSI+ononetin

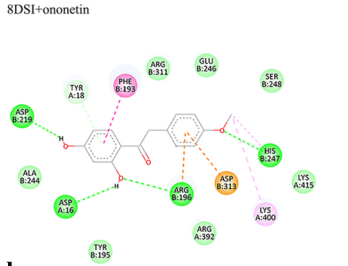

l.

8DSE+pacovatinin A

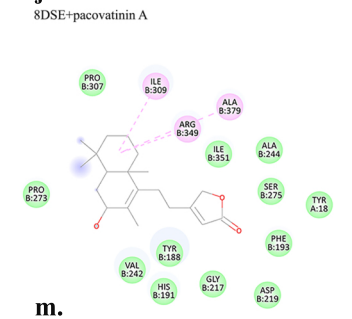

m.

7ENQ+pacovatinin B

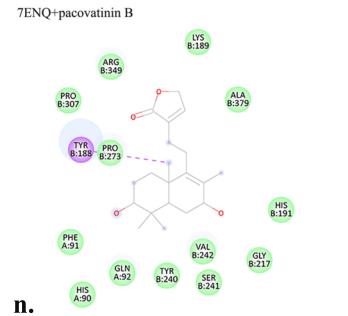

n.

7ENQ+pacovatinin C

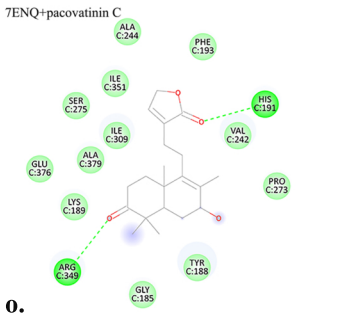

o.

8DSI+sesamolin

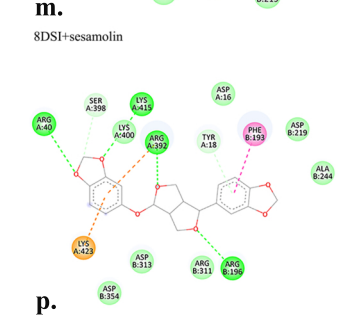

p.

7ENQ+stylopine

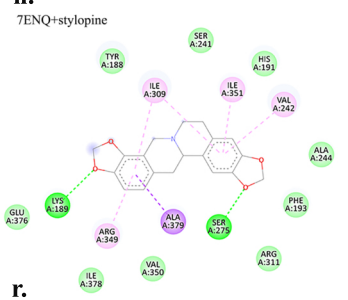

r.

- Van der Waals
- Conventional hydrogen
- π-cation
- π-anion
- Attractive charge
- π-sigma
- Amide-π stacked
- π-π stacked
- Carbon-hydrogen
- π-donor hydrogen
- Alkyl
- π-alkyl
- Unfavorable donor-donor

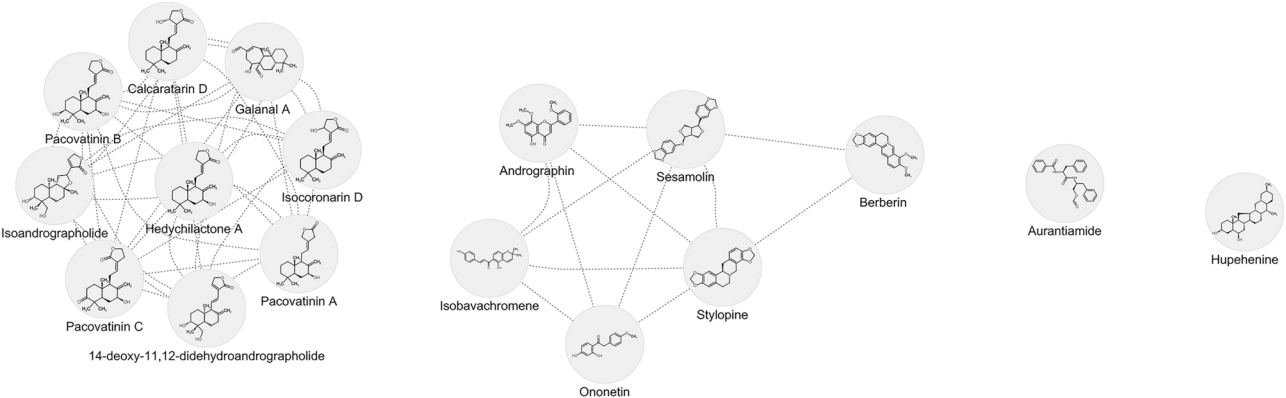
Calcaratarin D
Galanal A
Pacovatinin B
Isocoronarin D
Isoandrographolide
Hedychilactone A
Pacovatinin A
Pacovatinin C
14-deoxy-11,12-didehydroandrographolide
Andrographin
Sesamolin
Berberin
Aurantiamide
Hupehenine
Isobavachromene
Stylopine
Ononetin

Interaction sites of NAMPT modulators		Amino acids
Active site	**Nucleobase pocket**	Tyr-18
		Phe-193
	Doorsill	Asp-219
		Ser-241
		Val-242
		His-247
		Ser-275
	Rear channel	Gly-185
		Tyr-188
		Lys-189
		His-191
		Val-242
		Pro-272
		Thr-304
		Pro-307
		Arg-349
		Val-350
		Ile-351
		Ala-379

		Molecular docking scores (kcal/mol)					
Compound	**Molecular weight (g/mol)**	**8DSC**	**7ENQ**	**8DSE**	**8DSI**	**4o13**	**4N9C**
Andrographin	403	-8,6	-8,2	-8,2	-8,4	-9,5	-7,9
Aurantiamide	336	-10,4	-10	-10,2	-10,3	-10	-9,6
Berberine	318	-8,9	-9,4	-9,5	-9	-9,9	-9,6
Calcaratarin D	332	-9,6	-9,8	-9,9	-10	-9,6	-9,8
14-deoxy-11,12-didehydroandrographolide	318	-8,8	-8,9	-8,4	-8,4	-9,3	-9,5
Galanal A	318	-8,5	-9	-8	-8,1	-8,4	-8,4
Hedychilactone A	318	-9,2	-10,1	-9,8	-10,2	-8,3	-9
Hupehenine	416	-10	-10,7	-10	-9,9	-10,6	-10,1
Isoandrographolide	350	-9,1	-9,4	-8,9	-8,9	-8,9	-9,1
Isobavachromene	322	-10,7	-10,4	-11,1	-10,7	-11,8	-9,4
Isocoronarin D	318	-9,5	-9,5	-9,3	-9,4	-10,4	-9,7
Ononetin	318	-9,3	-8,9	-8,5	-9,4	-8,7	-8
Pacovatinin A	334	-9,7	-9,5	-9,7	-9,3	-9,8	-9,4
Pacovatinin B	332	-9	-9,4	-9,2	-8,9	-8,7	-9,1
Pacovatinin C	370	-9	-9,7	-9,2	-9,2	-9,6	-9,7
Sesamolin	323	-11,6	-10,8	-11,5	-11,8	-11,7	-10,3
Stylopine	322	-10,3	-11,2	-10,7	-9,9	-10,7	-10,4
Positive controls							
Activators, substrate and product:							
NAM	122	-6,8	-5,8	-6,7	-6,6	-6,6	-5,4
NAT-5r (HY-148948)	324	-8,5	-8,8	-8,6	-8,6	-9	-9
NMN	334	-9	-8,6	-8,5	-9,1	-9,4	-8,5
P7C3	474	-9,3	-9,7	-9,9	-9,6	-9,9	-8,7
Quercitrin	448	-10,3	-10,3	-10,6	-10,6	-10,4	-9,9
SBI-797812	403	-10,2	-9,6	-10,5	-11,1	-10,4	-9,3
TIE (NP-A1-R)	473	-10	-10,4	-10,6	-10,1	-11,6	-10,5
US11452717	262	-9,3	-9,4	-9,6	-9,6	-9,2	-8,1
ZN-2-43	537	-11,7	-11,6	-11,8	-11,8	-12,7	-10,7
Inhibitors:							
1QR	399	-10	-10,8	-10,1	-10,1	-9,5	-10,9

20M	505	-10,3	-11	-10,5	-10,5	-10,8	-10,3
C5V	397	-10,7	-11,1	-10,3	-10,2	-11,9	-10,3
FK866	392	-9,7	-9,8	-10	-10	-10,9	-8,9
GMX1778	372	-9,6	-8,2	-9,5	-9,6	-9,6	-8
GNE-617	427	-11,3	-10,8	-12,2	-11,5	-11,9	-10
GNE-618	460	-12,5	-11,1	-12,1	-12	-12,3	-10
Negative controls							
Acetylsalicylsalicylic acid	300	-8,6	-8,6	-8,3	-8,6	-8,7	-8
Maltose	342	-8	-8,1	-7,9	-8,4	-7,9	-8,3
Melitriose	504	-9,2	-9,2	-9,2	-9,1	-9,1	-9,2
Saccharose	343	-7,8	-7,6	-8,4	-7,8	-7,9	-7,7
Random control:							
Eszopiclone	389	-10,2	-9,5	-10,3	-9,7	-10,9	-9

Compound	Nucleobase pocket	Doorsill	Rear channel
GMX1778			
GNE-617			
GNE-618			
NAT-5R			
TIE			
ZN-2-43			
Acetylsalicylsalicylic acid			
Maltose			
Melitriose			
Eszopiclone			

Positive controls

Negative controls

Random control

All other types of interactions

Van der Waals interaction

No interaction observed

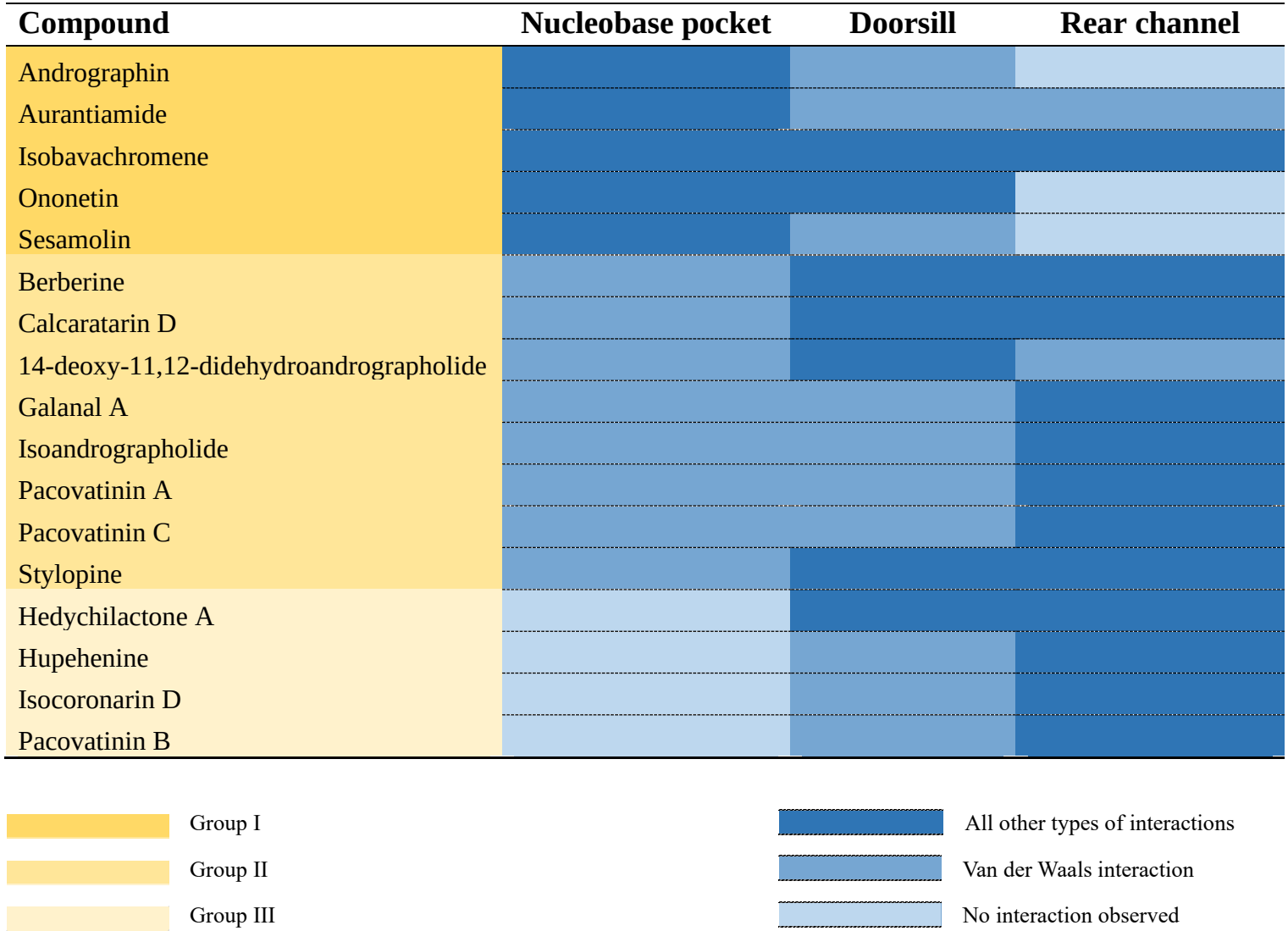
Compound
Nucleobase pocket
Doorsill
Rear channel
Andrographin
Aurantiamide
Isobavachromene
Ononetin
Sesamolin
Berberine
Calcaratarin D
14-deoxy-11,12-didehydroandrographolide
Galanal A
Isoandrographolide
Pacovatinin A
Pacovatinin C
Stylopine
Hedychilactone A
Hupehenine
Isocoronarin D
Pacovatinin B
Group I
Group II
Group III
All other types of interactions
Van der Waals interaction
No interaction observed